Colloid and Polymer Science (2024) 302:1–11
https://doi.org/10.1007/s00396-023-05173-3

RESEARCH

Investigating the effect of temperature, angular frequency, and strain on the rheological properties of shear thickening fluid (STF) with different weight fractions of fumed silica

Sajjad Astaraki[1] · Ehsan Zamani[1] · Majid Moghadam[2] · Mohammad Hossein Pol[3] · Hosein Hasannezhad[4]

Received: 14 August 2023 / Revised: 15 September 2023 / Accepted: 19 September 2023 / Published online: 28 September 2023

Abstract

Shear thickening fluids (STFs) have gained attention for their capacity to increase viscosity with higher shear rates, rendering them solid-like under high-impact conditions. This reversibility renders STFs valuable for diverse applications, particularly in defense systems. Preceding our study, mechanical hurdles, such as aggregation and blending issues, hindered efficient utilization. Our research presents an innovative method for STF synthesis using polyethylene glycol and SiO2 nanoparticles. Significantly, we employed a hot plate and oil bath to remove ethanol from the STF, a distinctive aspect of our approach. We also systematically explored the impact of temperature and the dispersion weight fraction of fumed silica nanoparticles on crucial rheological parameters, encompassing viscosity, shear rate, storage modulus (G′), and loss modulus (G″). As temperatures increased, the critical shear rate also rose, while viscosity decreased. Additionally, we observed a significant enhancement in thickening behavior with higher SiO2 concentrations in STFs. For instance, the peak viscosity of 15 wt% STF decreased by approximately 69.47% from 20 to 40 °C and by approximately 89.92% from 20 to 60 °C. This study highlights the unique rheological properties of STFs.

Keywords Nanoparticles · Polyethylene glycol · Rheological properties · Shear rate · Viscosity

Introduction

Colloidal suspensions called STFs increase in viscosity as shear rates increase [1–4]. As a result, STFs continue to behave as solid-like materials under high-impact loads. Reversibility is one of the most important properties of STFs, meaning they can be changed from solid back into a liquid by evacuating the connecting stretch. The rheological parameters of these "smart" fluids have been investigated for a long time to determine the application of these "smart" fluids in defensive systems. There were initial mechanical problems associated with thickening, including aggregation and overburdening blenders, thus restricting the rate of application [5–9]. Recent developments have utilized the interesting properties of these fluids to create more innovative materials and structures. It could be a colloidal liquid suspension where the shear rate is higher than the critical shear rate, and as a result, the viscosity increases significantly [11–14]. In general, colloidal structures present a scattered stage of a two-component structure whose dispersed phase is too small for the optical magnifying lens to be properly detected and can be influenced by other forces. When STFs are exposed to low shear or shear stresses, they frequently show a thinning behavior. The STF's viscosity becomes higher with greater shear stress as well as shifts gradually or simultaneously from shear thinning to shear thickening. It is called spasmodic thickening when the viscosity of STFs suddenly increases. A reversible change in viscosity occurs when shear stress decreases from the material, meaning the viscosity will decrease subsequently [6]. In shear thickening, colloids and suspensions are firmly inserted. In cases where they are unsettled at a low shear rate, such suspensions behave like lean liquids; however,

✉ Ehsan Zamani
zamani.ehsan@sku.ac.ir

1 Department of Mechanical Engineering, Shahrekord University, Shahrekord, Iran, P. O. Box 115

2 Faculty of Chemistry, University of Isfahan, Isfahan, Iran

3 Department of Mechanical Engineering, Tafresh University, Tafresh, Iran

4 Faculty of Mechanical Engineering, Sahand University of Technology, Tabriz, Iran

when they are unsettled at a high shear rate, they are incredibly thick. Despite this, expanded viscosity poses other challenges for STF industries. Due to this function, they make good dampers and shock absorbers. As a result of this flexibility, STFs are used to enhance the impact resistance of athletic hardware or fluid armor. The American Rheological Society teaches rheology, which is derived from the Greek rheos (work) and logos (science). Depending on their chemical and smaller-scale structures, all materials behave differently. Therefore, behavior control is a key component of commercial frameworks. Rheology kinematics are controlled by concepts. The analysis of kinematics provides geometrical angles of distortion and development, while the analysis of preservation law takes into account forces, the sharing of energy, stresses, and the diverse connections between body groups. This is where rheology comes into play, as it is the application of these logical standards and tests to solve problems relevant to polymer engineering, nourishment generation, printing, lubrication, and some other technologies [7, 8]. STFs have a great deal of potential in industries for integrating inside damper frameworks for optimizing their dynamic performance [9, 10]. In addition, dimples inside tubes can be used to enhance heat transfer in various applications, including heat exchangers [11–19]; in some cases, STFs are used in heat exchangers or cooling systems to improve their efficiency. The combination of dimples and STFs can potentially lead to even better heat transfer performance due to the enhanced fluid mixing caused by dimples and the unique rheological properties of STFs. Framework damage and vibration resistance are improved with the help of auxiliary parts [20–23]. The idea behind STFs is to constrain the mobility of the knees, shoulders, lower legs, and hips to block their rapid movement. Recent studies have shown that multiphase STF frameworks with nanoparticles within the suspensions would benefit from the addition of nanoparticles. One of the most important down-to-earth multiphase STFs is the MSTF, which is a combination of magnetorheological liquids and STFs [24]. Multiphase STFs were introduced several years ago with ceramic particles and carbon nanotubes. There has been evidence that these substances can alter the thickening behavior of STFs for defensive purposes [25–28]. In some studies, steady rheological properties and energetic rheological properties of STFs have been examined. Moreover, the rheological highlights have been discussed in terms of molecule measurement, surface charges, volume, strong stage, and the properties of the carrier fluid [29–32]. In accordance with [33], the length of nano-silica particles and polyethylene glycols is presented as a viable measurement of STF's flow properties. From the study findings, it was observed that the force between molecules varies according to the force levels experienced due to the presence of suspended silica nanoparticles in a carrier fluid. The majority of previous research has primarily focused on analyzing the rheological behavior of STFs at a temperature of 22 °C, with limited attention given to exploring how temperature affects STF properties during the processing phase. Consequently, it is crucial to understand how temperature influences STF behavior and microstructure. Several studies have demonstrated that STF can be made by scattering solid-phase particles in polyethylene glycol and polypropylene glycol, which could be an example of STF. According to [23, 25, 34–37], colloidal suspension rheology is highly dependent on interparticle forces and the nanoscopic properties of colloidal surfaces.

In this study, the rheological properties of thickened fluid were investigated using polyethylene glycol 400 and silica fume. It has been tried to pay attention to a large number of rheological properties of this fluid, which have not been fully paid in one place in previous research. Rheology is crucial for explaining the forces that act between suspended particles on the nanoscale. Mechanical mixing and high-speed ultrasound were used to disperse fumed silica particles in polyethylene glycol based on various loadings to prepare STF. The innovative aspect of this research is the method of making STF, which is unique to this research. To make STF, a hot plate heating method has been used while stirring the materials to evaporate ethanol so that the materials are placed in the oil bath at a temperature of 80 °C. This action helps the evaporation of alcohol from the fluid, and due to the presence of temperature and the reduction of viscosity, it makes stirring easier and causes a better formation of chemical bonds between the components of the STF.

Experimental

Materials and STF synthesis

As a result of the fullness of silanol bunches on the surfaces of carbonized SiO_2 particles, they appear to be hydrophilic. In a hydrogen/oxygen fire, fumed silica nanoparticles are synthesized through the hydrolysis method and tetrachlorosilane at high temperatures [37]. In this study, hydrophilic SiO_2 (Aerosil 200 measuring 12 nm in diameter) was acquired from Degussa Company. Polyethylene glycol (trademark PEG400) was provided via Merck containing an atomic weight of 400 (g/mol) and ethanol with a purity of 99.5% was used. Table 1 shows the properties of applied materials for preparation of STF. Figure 1 shows the materials prepared for the production of STF. In Table 1, samples with different weight fractions are named. Table 2 shows the weight fraction of the fumed SiO_2/PEG suspensions.

Table 1 Properties of applied materials

Materials	Density (g cm^{-3})	Mollar mass (g mol^{-1})	Formula
PEG	1.13	380–420	$C_{2n}H_{4n+2}O_{n+1}$
Silica	2.2	60.09	SiO_2
Ethanol	0.789	46.068	C_2H_6O

Table 2 The weight fraction of the fumed SiO_2/PEG suspensions

Sample (fumed SiO2+PEG400)	The weight fraction of the fumed silica (wt%)
A	15
B	25
C	35

Preparation of STFs

An ultrasonication process and mechanical blending were used to fabricate the STF. The synthesized STFs in this experiment include concentrations of 15%, 25%, and 35%. The following steps (A–G) were carried out to fabricate the samples, and in Fig. 2, a view of the production of STFs is shown.

(A) Fumed SiO_2 was hydrophilic and sensitive to humidity adsorption. To remove moisture from fumed silica, the material was first heated to 60 °C in a vacuum oven for 24 h.
(B) Direct mixing of fumed silica with ethanol by a mechanical stirrer at a speed of 5000 rpm at room temperature (Three to one is the weight ratio of ethanol to STF).
(C) As a result of ultrasound sonication, particles in suspension can be distributed more evenly within the suspension by reducing their aggregation [38]. This was achieved by sonicating the resulting fumes with ethanol for 3 h in 0.5 cycles at 30% amplitude with a horn tip sonicator (Hielscher-UP400S).
(D) By magnetic stirrer for 18 h at room temperature, polyethylene glycol 400 is mixed continuously with SiO_2/ethanol solution.
(E) STF sonicated for 5 h in 0.5 cycles and 30% amplitude.
(F) The STF was mixed for 8 h by a mechanical stirrer at 10,000 rpm. A 50-ml glass beaker experiment container was used during for the purpose. At this stage, to remove excess alcohol from STF, it was heated in an oil bath at 80 °C by a hot plate. It was observed that at this temperature, excess alcohol was removed to a very significant extent. And the stirring became much easier and the number of bubbles trapped in STF was less compared to the studies that put STF in the oven and the bubbles came out faster due to the heat generated and the viscosity reduction.
(G) To remove bubbles from the STF, the specimen was vacuumed at 22 °C for 10 h.

Rheological test

A rheometer is one of the most widely used tools for measuring fluid rheological properties. Rotary rheometer testing was carried out on a parallel plate rheometer (MCR 301, Anton Paar) in both static and dynamic shear conditions as a function of angular frequency. STF was filled sufficiently on the test disc by using a geometry with a 20 mm diameter and 0.8 mm gap (PP-20). In 20 °C conditions, viscosity was measured in the 0.1–1000 s^{-1} range depending on the shear rate [39, 40]. In the temperature sweep test, the frequency sweep, and Oscillatory Strain Amplitude Sweep, the test geometry conditions have not changed (Fig. 3).

(a) (b) (c)

Fig. 1 The material used is **a** polyethylene glycol 400, **b** ethanol, and **c** fumed silica particles

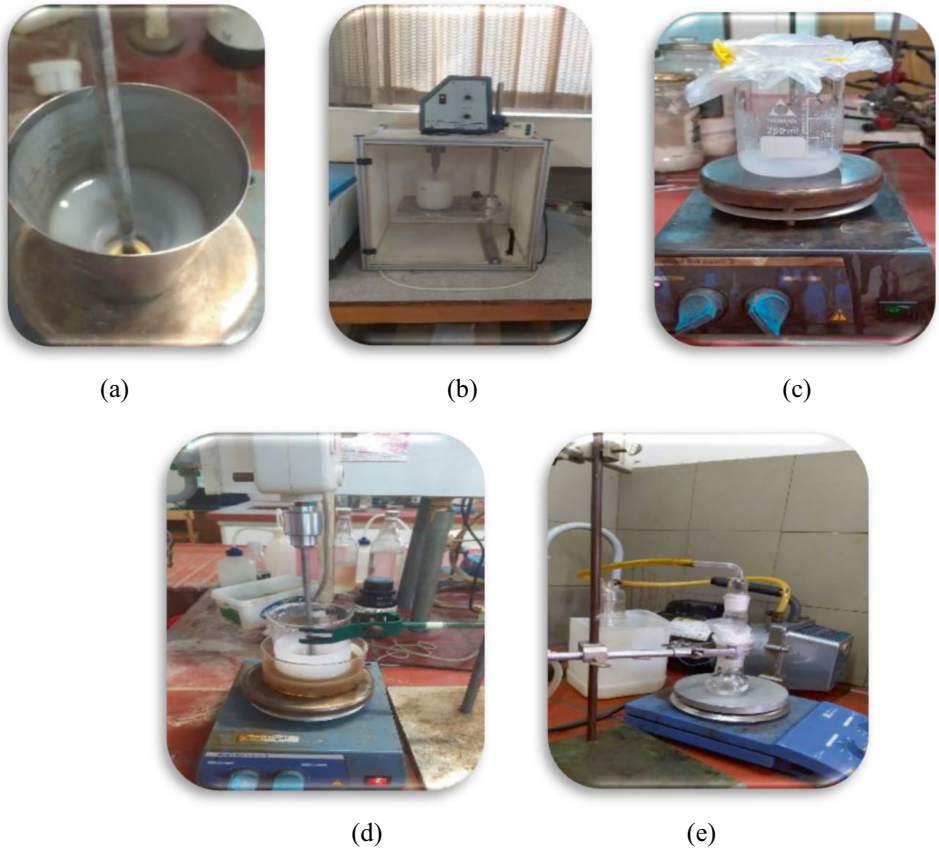

Fig. 2 Steps of the STF preparation: **a** mechanical blending of fumed silica with ethanol, **b** sonication of fumed silica with ethanol, **c** mixing of PEG400 with fumed silica and ethanol solution by a magnetic stirrer, **d** the STF was mixed in an oil bath by a mechanical stirrer for 8 h, **e** the sample was placed under vacuum

Results and discussion

Shear thickening characteristics of fumed SiO2/PEG400

A standard deviation of less than 5% was found in the reported results. Upon reducing the loading of fumed silica particles, some independent SiO_2 aggregates are formed. Consequently, the STF's viscosity decreases further, resulting in shear-thinned behavior. Due to the increased shear rate, hydrodynamic lubrication forces overcome other forces in the suspension, leading to more fumed SiO_2 aggregates being formed.

The viscosity of the shear flow fluctuates based on the shear rate. Figure 4 depicts the influence of silica weight fraction on viscosity. According to the results, all samples exhibit similar rheological behavior regardless of the fumed SiO_2 concentration; viscosity decreases slightly with a rising shear rate and exhibits shear thinning behavior. In response to an increase in shear rate, the viscosity increases dramatically, and shear thickening behavior is demonstrated, and it reaches its maximum value. Then, in the presence of a further increase in shear rate, the viscosity starts to decrease. Attempting to explain this shear thickening behavior, Bossis and Brady proposed a theory based on the Stokesian hydrodynamic model called "hydro clusters" [41, 42]. As a result

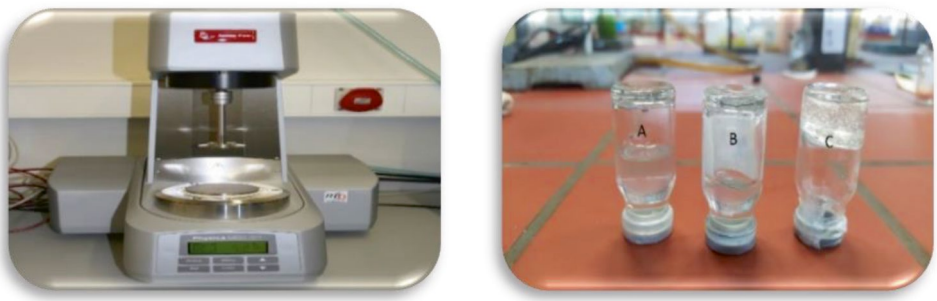

Fig. 3 **a** Rheometer (MCR 301, Anton Paar), **b** samples prepared with A = 15%, B = 25%, and C = 35% weight fractions

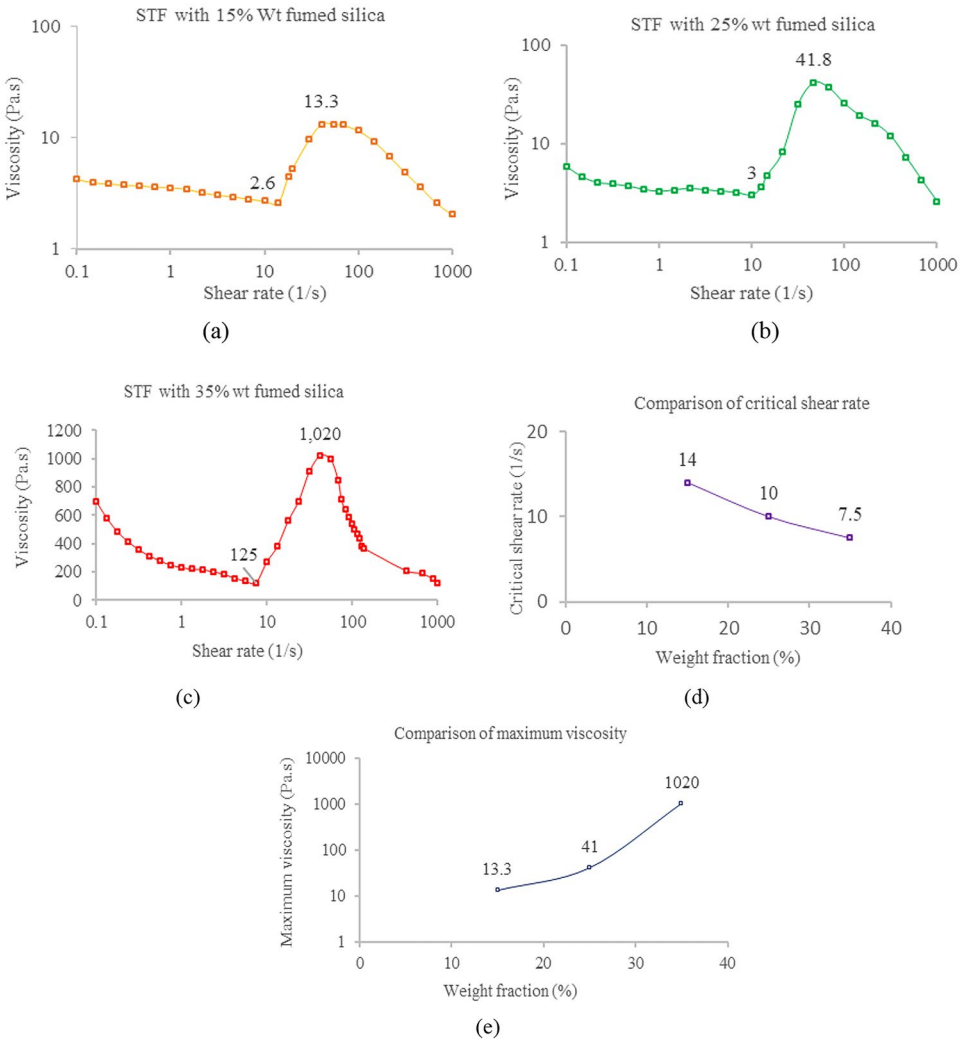

Fig. 4 **a**–**c** Curve of viscosity—the shear rate in weight fraction of 15, 25, and 35%, **d** curve of critical shear rate-weight fraction, and **e** curve of maximum viscosity-weight fraction

of the terminal hydroxyls on polyethylene glycol molecules and the abundance of silanol groups on fumed silica, hydrogen bonds can easily be formed between them. As a solvation layer, polyethylene glycol molecules are deposited on fumed silica surfaces by hydrogen bonds. Fumed SiO_2 dispersion in sol is stabilized by this effect since the particles are prevented from interacting. Consequently, the viscosity is altered. As the shear-rate increases, the system fails in its capability to recover, damage increases, and hydro clusters are formed when small fumed silica aggregates collide. The big "hydro clusters" can act like walls and hinder fluid flow. The system's viscosity increases steeply as a result.

Temperature effects on STF characteristics

The obtained results have less than a 5% standard deviation. Figure 5 compares the impact of temperatures of 20, 40, and 60 °C on the viscosity of SiO_2/PEG400 at a constant weight fraction of 15% silica fume. Although this fluid showed ST behavior in this temperature range, the viscosity of particles at 60 °C is substantially less than at 40 °C and 20 °C. As temperatures increase, the Brownian motion of the molecules increases and leads to a very irregular structure. A second effect of rising temperature is the weakening of the interparticle hydrogen bond and solvent vapors. Figure 5 illustrates how the cutting rate in shear thickening occurs because shear thickening primarily occurs as hydrodynamic lubrication happens. The forces defeat the interparticle repulsive forces and cause their formation. At higher temperatures, "hydro clusters" are also repelled by stronger forces, so shear rates need to be increased to induce their formation. In general, critical shear rates increase as temperature increases [43].

Temperature-induced gelation of fumed silica/PEG400

The temperature response of storage modulus (G″) and loss modulus (G′) at concentrations of 15, 25, and 35% by weight is shown in Fig. 6. This suggests that high temperatures alter

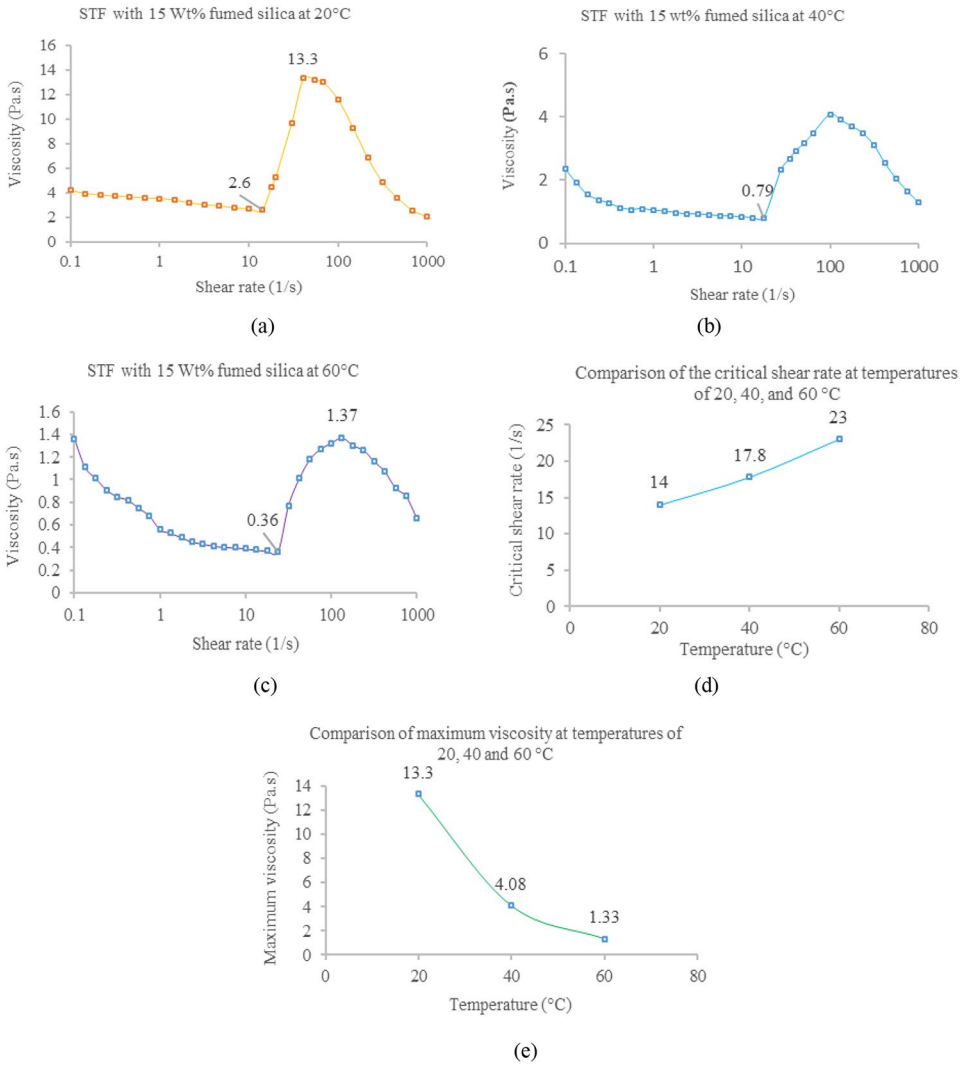

Fig. 5 **a**–**c** Curves of viscosity-temperatures fumed SiO_2/PEG400 (at a concentration of 15 wt% at different temperatures (20 °C, 40 °C, and 60 °C), **d** comparison of the critical shear rate at temperatures of 20, 40, and 60 °C, and **e** comparison of maximum viscosity at various temperatures

the structure of SiO_2/PEG400. As part of the analysis of the samples, dynamic frequency sweeps were conducted on the samples to further examine the structure change. As is depicted in Fig. 7, G′ and G″ become larger with increasing frequency. Polyethylene glycol molecules are absorbed onto fumed silica by hydrogen bonding. They serve as a solvent layer preventing interparticle interaction and causing efficient distribution of the silica foam particles. High temperatures create an irregular structure in the fluid. This reduces the solubility in the solvent layers and decreases the storage and loss modulus [44–46].

The test temperature was first raised from 10 to 80 °C at a rate of 5 °C per minute. According to the "hydro clusters" theory, the hydrodynamic lubrication forces in the shear thickening mechanism, the polyethylene glycol molecules, and fumed SiO_2 particles have a high tendency to form hydrogen bonds. It covers the particles with a layer of solvent. This prevents particle interaction and facilitates particle dispersion in the solvent. Polyethylene glycol molecules become more mobile as the temperature rises due to the weakening of hydrogen bonds between particles and solvents. It has led to the weakening of the solubility layer on the surface of the particles. In response to the temperature increases, the solubility layer covering the particles slowly disappears. The particles are gradually released from interactions between solid particles and liquid solvents. The presence of many silanol groups in the particles increases the probability of Brownian motion colliding, forming hydrogen bonds around their surfaces. The formed "hydro clusters" are connected, and they can act as a barrier and significantly impede fluid flow, resulting in thickened shear behavior.

Oscillatory strain amplitude sweep behavior of fumed SiO_2/PEG400

Under multiple deformations of strain amplitude sweep experiments, complex fluids can be investigated for their

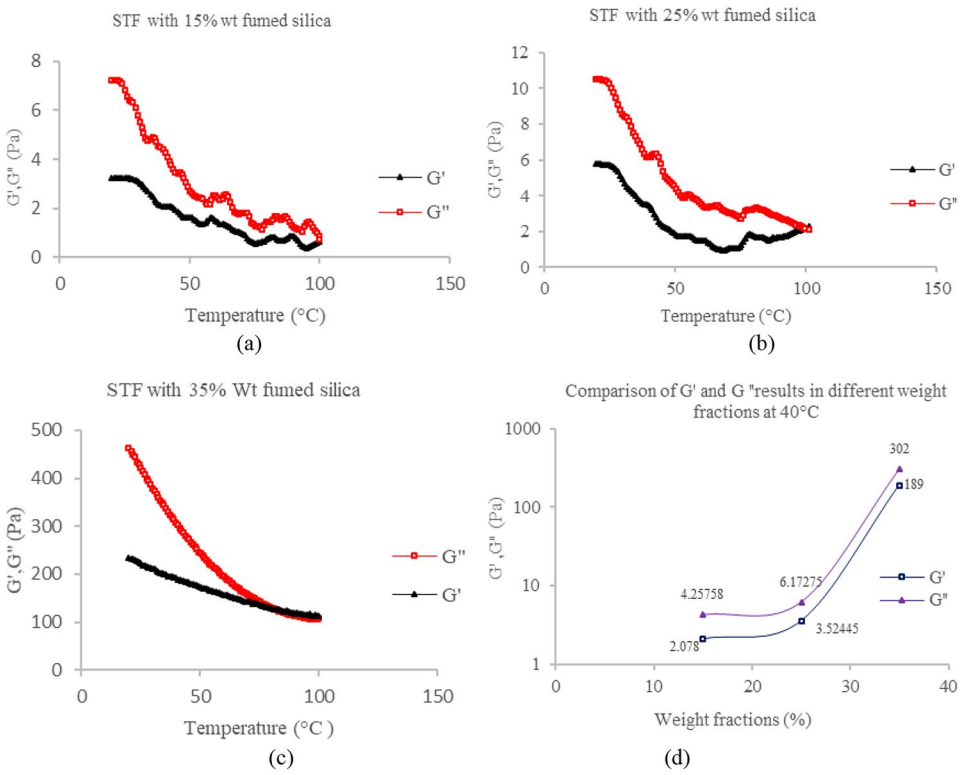

Fig. 6 **a**–**c** Temperature sweeps for fumed SiO2/PEG400 at weight fractions of 15, 25, and 35%, **d** comparison of G′ and G″ results for different weight fractions at 40 °C. The test was performed in the strain range of 0.2% and fixed frequency of 1 rad/s

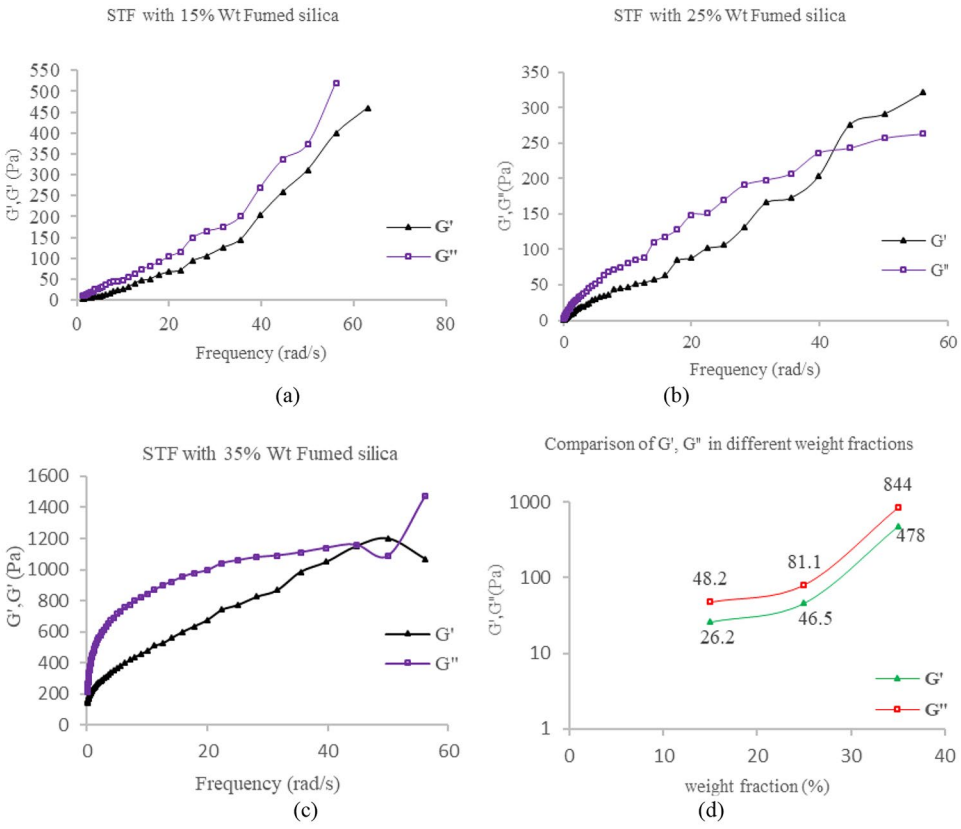

Fig. 7 **a**–**c** The frequency sweep for fumed SiO_2/PEG400 at 15, 25, and 35% weight fractions, **d** comparison of G′ and G″ in different weight fractions. It was done at 10 rad/s

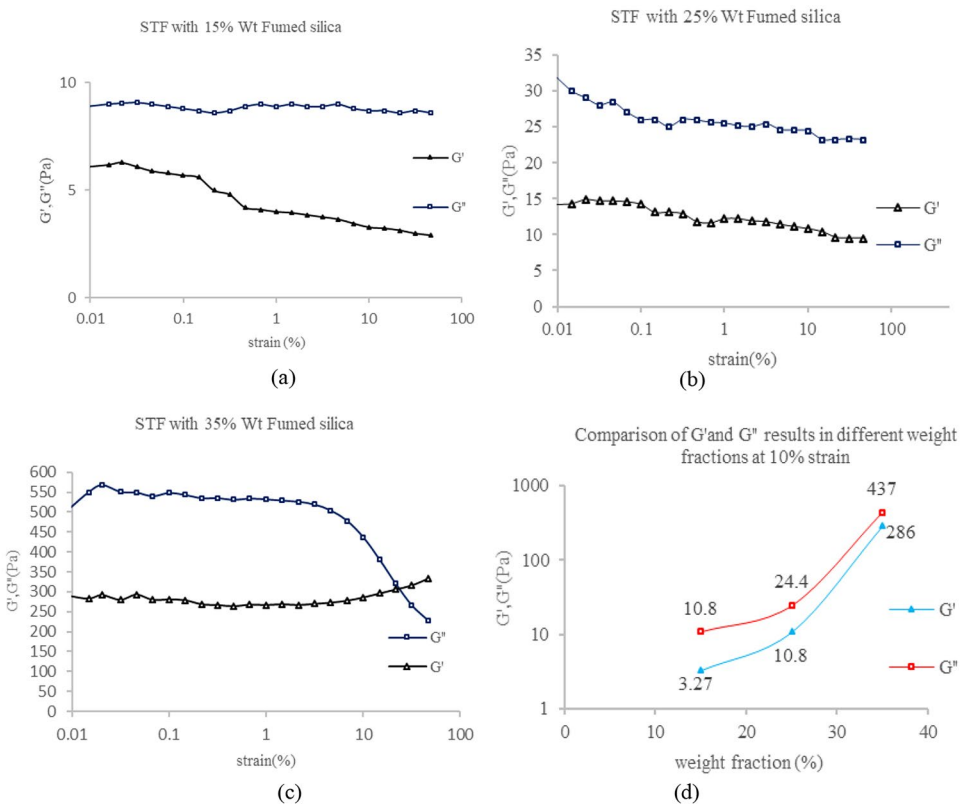

Fig. 8 **a**–**c** Oscillatory strain amplitude sweep response of silica/PEG, including various weight fractions of silica, and **d** comparison of G′ and G″ results in different weight fractions at 10% strain at 10 rad/s and 20 °C

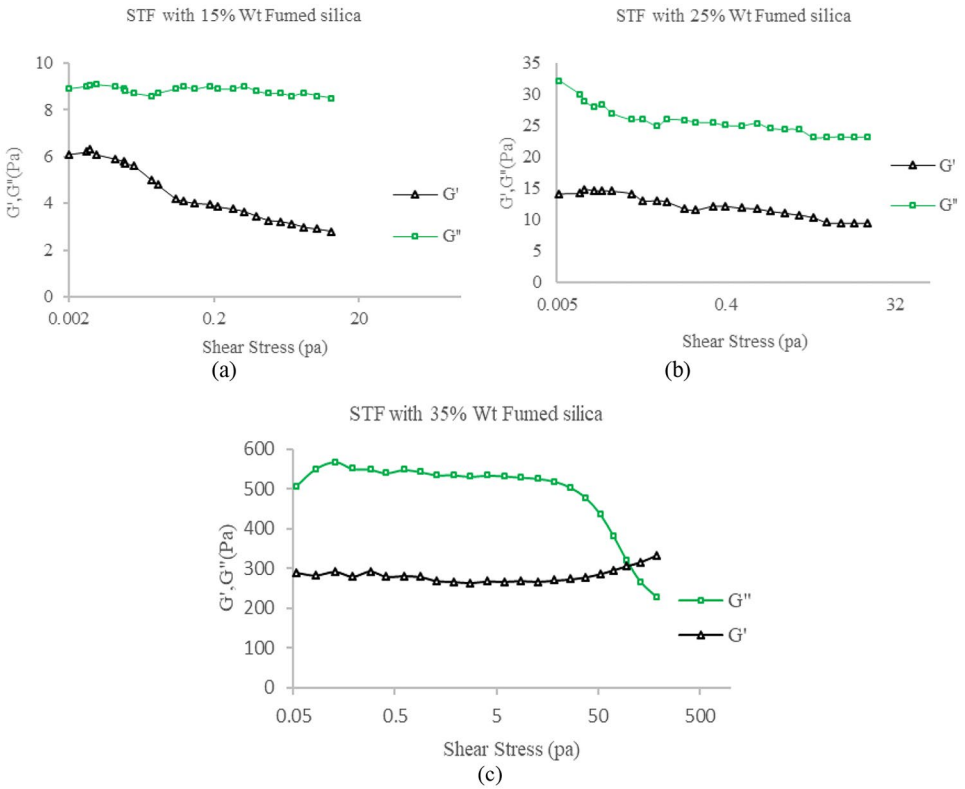

Fig. 9 **a**–**c** G′ and G″—shear stress curves extracted from the sample tested by the oscillatory strain amplitude method, STF including various weight fractions of silica at 1 rad/s and 20 °C

nonlinear viscoelastic properties and microstructure formation [47]. Figure 8 shows the sweep response of the oscillatory strain range of STFs for three categories of weight fractions. In the weight fractions of 15 and 25%, the material behaves more liquidly. As the weight fraction increases up to 35%, they become closer to solids. In all three cases, the weight fraction has decreased with the increase in the strain of G′ and G″. Which shows molecular disintegration [48]. As shown in Fig. 8 G′ 35% wt > G′ 25% wt > G′ 15% wt.

With increasing strain, the hydrogen bond between fumed silica molecules and polyethylene glycol weakens and causes the material to change from a solid to a liquid state. As shown in the weight fraction of 35%, G′ and G″ are equal. [49]. This value agrees with Ball's prediction, assuming that the clusters form a fractal network [50]. This study verified the frequency characteristics of the specimens by examining the oscillatory shear response of the strain amplitude. The sample with a weight fraction of 35% has a dominant elastic response in the linear region, which indicates a strong network structure. Based on Fig. 9, a displacement method of fluctuating strain range of the weight fraction of fumed silica nanoparticles has been found to increase the shear stress of a sample by increasing the concentration of the samples up to 35% weight fraction in the test conditions. In the diagram shown in Fig. 9, G′ and G″ have decreased with the increase in stress and strain. The results obtained in Fig. 9 show that G′ 35 wt% > G′ 25 wt% > G′ 15 wt%.

Conclusions

In this study, the shear thickening properties of STF solution and the influence of temperature on structure formation were analyzed. Temperature and dispersion weight fraction of fumed silica nanoparticles were investigated to determine their effects on viscosity, shear rate, storage modulus (G′), and loss modulus (G″). Fumed silica SiO_2 particles carry abundant silanol groups on their surface and have a branched chain structure. When silica is dispersed in polyethylene glycol, an STF is formed. The results revealed that STF can exhibit significant thickening characteristics due to hydrocluster formation caused by hydrodynamic lubrication forces.

As the temperature rises, the critical shear rate where shear thickening occurs increases. Also, with increasing the temperature, STF's viscosity decreases. A complete comparative rheological analysis of STFs showed a significant increase in thickening behavior in STFs with higher SiO_2 concentrations. The peak viscosity of 15 wt% STF decreased by approximately 69.47% from 20 to 40 °C and by approximately 89.92% from 20 to 60 °C. As the temperature rises, the critical shear rate where shear thickening occurs increases. The critical shear rate of 15 wt% STF decreased by approximately 27.14% from 20 to 40 °C and by approximately 64.29% from 20 to 60 °C. Increasing the solid phase weight fraction increases the viscosity. The results showed that the storage modulus (G″) and loss modulus (G′) increase with increasing the weight fraction. However, as the temperature increases from 20 to 80 °C, the values of G′ and G″ decrease. Oscillatory Strain Amplitude Sweep Response of STF for three types of weight distribution showed G′ 35 wt% > G′ 25 wt% > G′ 15 wt%. So, the value of G′ for STF at 15 wt% decreased by approximately 43.68% compared to 25 wt%, and it decreased by approximately 94.48% compared to 35 wt%. Furthermore, the value of G″ for STF at 15 wt% decreased by approximately 40.57% compared to 25 wt%, and it decreased by approximately 94.33% compared to 35 wt%.

Author contribution Sajjad Astaraki: Preparing samples and testing, Methodology, writing – original draft, investigation. Ehsan Zamani: Supervision, writing – review & editing, project administration. Majid Moghadam: Conceptualization, validation. Mohammad Hossein Pol: Formal analysis, review. Hosein Hasannezhad: Review & editing.

Availability of data and materials Data and materials will be available upon request.

Declarations

Ethics approval and consent to participate Not applicable.

Competing interests The authors declare no competing interests.

References

1. Boersma WH, Laven J, Stein HN (1990) Shear thickening (dilatancy) in concentrated dispersions. AIChE J 36:321–332
2. Lee YS, Wagner NJ (2006) Rheological properties and small-angle neutron-scattering of a shear thickening, nanoparticle dispersion at high shear rates. Ind Eng Chem Res 45:7015–7024
3. Wagner NJ, Brady JF (2009) Shear thickening in colloidal dispersions. Phys Today 62:27–32
4. Lee YS, Wagner NJ (2003) Dynamic properties of shear thickening colloidal suspensions. Rheol Acta 42:199–208
5. Hasannezhad, H, Yazdani M (2022) Investigate the dynamic compressive (cushioning) response of 3D GFRP composites when the STF matrix base material is modified PEG, J Mol Liq 366:120304. https://doi.org/10.1016/j.molliq.2022.120304
6. Yu M, Qiao X, Dong X et al (2018) Effect of particle modification on the shear thickening behaviors of the suspensions of silica nanoparticles in PEG. Colloid Polym Sci 296:1767–1776
7. Shende T, Joekar-Niasar V, Babaei M (2021) An empirical equation for shear viscosity of shear thickening fluids 325:115220–115220. https://doi.org/10.1016/j.molliq.2020.115220
8. Islam E, Kaur G, Bhattacharjee D et al (2018) Effect of cellulose beads on shear-thickening behavior in concentrated polymer dispersions. Colloid Polym Sci 296:883–893

9. Mohsen Jeddi M, Yazdani Hossein Hasannezhad (2021) Experimental study on puncture resistance of 2D and 3D glass fabrics reinforced with shear thickening fluid (STF). https://doi.org/10.22060/ajme.2021.19920.5973
10. Guo F, Xu Z, Gu J (2023) Effects of nano-fumed silica and carbonyl iron powder of different particle sizes on the rheological properties of shear thickening fluids. Colloid Polym Sci 301:539–555
11. Arun M, Sivagami SM, Raja Vijay T, Vignesh G (2023) Experimental investigation on energy and exergy analysis of solar water heating system using zinc oxide-based Nanofluid. Arab J Sci Eng 48(3):3977–3988
12. Munusamy A, Barik D, Sharma P, Medhi BJ, Bora BJ (2023) Performance analysis of parabolic type solar water heater by using copper-dimpled tube with aluminum coating. Environ Sci Pollut Res 9:1–6
13. Barik D, Saeed MA, Ramachandran T (2022) Experimental and computational analysis of aluminum-coated dimple and plain tubes in solar water heater system. Energies 16(1):295
14. Arun M, Barik D, Sridhar KP (2022) Experimental and CFD analysis of dimple tube parabolic trough solar collector (PTSC) with TiO2 nanofluids. J Therm Anal Calorim 8:1–8
15. Arun M, Barik D, Sridhar KP, Dennison MS (2022) Thermal performance of a dimpled tube parabolic trough solar collector (PTSC) with SiO2 nanofluid. Int J Photoenergy 28:2022
16. Arun M, Barik D, Sridhar KP, Vignesh G (2022) Performance analysis of solar water heater using Al 2 O 3 nanoparticle with plain-dimple tube design. Exp Tech 1–4
17. Arun M, Barik D, Sridhar KP, Vignesh G (2021) Experimental and CFD analysis of artificial dimples surface roughness by using application of domestic solar water heater. In Intelligent Manufacturing and Energy Sustainability: Proceedings of ICIMES 2020 285–298. Springer Singapore.
18. Arun M, Barik D, Sridhar KP, Vignesh G (2021) Experimental and CFD analysis of plain and dimples tube at application of solar water heater. Materials Today: Proceedings 1(42):804–809
19. Arun M, Barik D, Sridhar KP, Vignesh G (2021) Experimental and CFD analysis of copper plain and dimples tube at application of solar water heater. Materials Today: Proceedings 1(42):410–415
20. Hasan-nezhad H, Yazdani M, Jeddi M (2022) High- and low-velocity impact experiments on treated STF/3D glass fabrics, Thin-Walled Struct 171:108720. https://doi.org/10.1016/j.tws.2021.108720
21. Bing Liu, Chengbin Du, Huaxia Deng, Yankai Fu, Fei Guo, Ling Song, Xinglong Gong (2022) Study on the shear thickening mechanism of multifunctional shear thickening gel and its energy dissipation under impact load. Polymer 247:124800. https://doi.org/10.1016/j.polymer.2022.124800
22. Jeddi M, Yazdani M, Hasan-nezhad H (2021) Energy absorption characteristics of aluminum sandwich panels with Shear Thickening Fluid (STF) filled 3D fabric cores under dynamic loading conditions. Thin-Walled Struct 168:108254. https://doi.org/10.1016/j.tws.2021.108254
23. Hasan-nezhad H, Yazdani M, Salami-Kalajahi M, Jeddi M (2020) Mechanical behavior of 3D GFRP composite with pure and treated shear thickening fluid matrix subject to quasi-static puncture and shear impact loading. J Compos Mater 54(26):3933–3948
24. Zhang X, Li W, Gong X (2010)Thixotropy of MR shear-thickening fluids. Smart Mater Struct 19:125012
25. Hasan-nezhad H, Yazdani M, Akbari A, Salami-Kalajahi M, Kalhori M-R (2022) Study the effects of PEG modification methods on the resistance of 3D E-glass woven-STF composites at quasi-static and low-velocity impact loads. J Mol Liq 362:119781
26. Gürgen S, Li W, Kus¸han MC (2016) The rheology of shear thickening fluids with various ceramic particle additives. Mater Des 104:312–9
27. Hasanzadeh M, Mottaghitalab V, Babaei H, Rezaei M (2016) The influence of carbon nanotubes on quasi-static puncture resistance and yarn pull-out behavior of shear-thickening fluids (STFs) impregnated woven fabrics. Compos PartAppl Sci Manuf 88:263–271
28. Petel OE, Ouellet S, Loiseau J, Frost DL, Higgins AJ (2015) A comparison of the ballistic performance of shear thickening fluids based on particle strength and volume fraction. Int J Impact Eng 85:83–96
29. Tan VBC, Tay TE, Teo WK, Solids J (2005) Struct 42: 1561–1576
30. Gómez-Merino AI, Jiménez-Galea JJ, Rubio-Hernández FJ, Arjona-Escudero JL, Santos-Ráez IM (2020) Heat transfer and rheological behavior of fumed silica nanofluids. Processes 8:1535. https://doi.org/10.3390/pr8121535
31. Abdi Esmaeil, Ata Khabaz-Aghdam, Hosein Hasan-nezhad, Bashir Behjat EAS, Marques, Yongming Yang, da Silva LFM (2022) The effect of graphene and graphene oxide on defective single lap adhesively bonded joints. J Compos Mater 56(17):2665–2675
32. Jiang WQ, Ye F, He QY, Gong XL, Feng JB, Lu L, Xuan SH (2014) J Colloid Interface Sci 413:8–16
33. Jiang T, Zukoski CF (2012) Macromolecules 45:9791–9803
34. Raghavan SR, Khan SA (1997) J Colloid Interface Sci 185:57–67
35. Raghavan SR, Walls HJ, Khan SA (2000) Langmuir 16:7920–7930
36. Kamibayashi M, Ogura H, Otsubo Y (2008) J Colloid Interface Sci 321:294–301
37. Gun'Ko VM, Mironyuk IF, Zarko VI, Voronin EF, Turov VV, Pakhlov EM, Goncharuk EV et al. (2005) Morphology and surface properties of fumed silicas. J Colloid Interface Sci 289(2):427–445
38. Haris A, Lee HP, Tan VB (2018) An experimental study on shock wave mitigation capability of polyurea and shear thickening fluid-based suspension pads. Def Technol 14(1):12–18
39. Chauhan RR, Dullens RPA, Velikov KP, Aarts DGAL (2017) Exploring concentration, surface area, and surface chemistry effects of colloidal aggregates on fat crystal networks. RSC Adv 7:28780–28787
40. Aliabadian E, Sadeghi S, Kamkar M, Chen Z, Sundararaj U (2018) Rheology of fumed silica nanoparticles/partially hydrolyzed polyacrylamide aqueous solutions under small and large amplitude oscillatory shear deformations, J Rheol 62:1197-1216
41. Kang TJ, Hong KH, Yoo MR (2010) Fiber Polym 11:719–724
42. Bossis G, Brady JF (1989) J Chem Phys 91:1866–1874
43. Suh YJ, Ullmann M, Friedlander SK, Park KY (2001) J Phys Chem B 105:11796–11799
44. Khan SA, Zoeller NJ (1993) J Rheol 37:1225–1235
45. Srinivasa R, Raghavan Walls HJ, Saad Khan* A (2000) Rheology of silica dispersions in organic liquids: new evidence for solvation forces dictated by hydrogen bonding, Langmuir 16:7920–7930
46. Liu X-Q, Bao R-Y, Wu X-J, Yang W, Xie B-H, Yang M-B (2015) Temperature induced gelation transition of a fumed silica/PEG shear thickening fluid. RSC Adv 5:18367–18374. https://doi.org/10.1039/c4ra16261g
47. Kyu H, Heun KS, Hyun AK, Jong LS (2002) Large amplitude oscillatory shear as a way to classify the complex fluids. J Non-newton Fluid Mech 107:51–65
48. Huang Qiang Gu, Mingyuan Sun Kang, Yanping J (2002) Effect of pretreatment on rheological properties of silicon carbide aqueous suspension. Ceram Int 28: 747–754
49. Shih W-H, Shih WY, Kim S-I, Liu J, Aksay IA (1990) Scaling behavior of the elastic properties of colloidal gels. Phys Rev A 42:4772

50. Richard Buscall P, Mills DA, Goodwin JW, Lawson DW (1988) Scaling behavior of the rheology of aggregate networks formed from colloidal particles. J Chem Soc Faraday Trans 1(84):4249–4260.